Hindawi
International Journal of Photoenergy
Volume 2021, Article ID 9940862, 15 pages
https://doi.org/10.1155/2021/9940862

Research Article

Active Power Management for PV Systems under High Penetration Scenario

Fernando Medina[1], **Nimrod Vazquez**[1], **Joaquín Vaquero**[2], **Jaime Arau**[3], **Leonel Estrada**[4] and **Elso Rodriguez**[1]

[1]*Electronics Engineering Department, TecNM-Instituto Tecnológico de Celaya, 38010 Celaya, Mexico*
[2]*Electronics Technology Area, Rey Juan Carlos University, 28933 Mostoles, Madrid, Spain*
[3]*Electronics Department, Tecnológico Nacional de México-Cenidet, 63490 Cuernavaca, Mexico*
[4]*Electronics Department, Instituto Tecnológico Superior del Sur de Guanajuato, 38980 Uriangato, Mexico*

Correspondence should be addressed to Nimrod Vazquez; n.vazquez@ieee.org

Received 25 March 2021; Accepted 23 May 2021; Published 4 June 2021

Academic Editor: Kumarasamy Sudhakar

Although PV systems are one of the most widely used alternatives as a renewable energy source due to their well-known advantages, there are significant challenges to address related to voltage fluctuations and reverse power flow caused by high PV penetration scenarios. As a potential solution to this problem, an active power management strategy is proposed in this work using a residential cluster as a benchmark. The proposed strategy is analyzed and experimentally verified, offering a simple way to reduce the voltage fluctuations by regulating the active power delivered by the PV system, achieving also relevant functionalities for the system, such as the regulation of the DC bus voltage, maximum power point tracking (MPPT), synchronization with the grid voltage, detection of high penetration conditions, and a simple strategy for the main controller with an effective performance. The proposal system shows satisfactory results being able to maintain grid voltage fluctuations within the voltage standard specifications.

1. Introduction

The number of photovoltaic (PV) systems connected to the electric grid has grown considerably in recent decades. It is estimated that the demand for PV systems will maintain its growth for the coming years. According to the International Energy Agency, by 2050, solar PV power generation will be around 16% of the world's electricity [1]. The fastest-growing areas of electricity production from PV systems are in the low-voltage (LV) grid that corresponds to the private and residential sectors.

The ease of connecting PV systems to the grid is an important factor for their growth, but also the availability of the technology, which allows users to install them quickly and easily. The distributed generation (DG) based on PV systems is currently high and increases every day; e.g., the installed capacity in Australia and Germany in recent years has increased by 80% and 99%, respectively [2–5], while in Europe, it was estimated at 49% [6]. Some of the benefits of using PV systems to improve the quality of the power grid are the reduction of losses and maintenance cost, as well as, of course, significant savings in the electricity billing for the end-user.

However, the massive use of grid-connected PV systems may affect the power quality; this is known as high PV penetration [7–9]. Some first cases of problems due to high penetration scenarios were reported in European countries such as Germany [10], the Netherlands [11], and the United Kingdom [12]. The electrical grid under a high PV penetration scenario should have variations in frequency and voltage levels [13, 14]. Different studies deal with the effects of high PV penetration into the electric grid [15–20]. The most

important effect is the variation in the voltage level [15–21]. The relevance of this problem is that the safe operating area of sensitive electronic equipment such as computers or medical devices may be lost [22].

In recent years, different techniques associated with voltage regulation and control methods to mitigate the effect of high PV penetration have been proposed. These solutions include studies to determine the maximum loads connected to the grid [23], grid layout and loads residential design [24], variable tap transformers [25] and smart transformers applications [26], battery bank systems [27–29], inverters with reactive power capability [30–33], and the interconnectivity of external devices with the grid as smart electrical vehicles [34]. Additionally, the theoretical use of a communication network that allows making decisions based on grid variations has been suggested [35].

Since the deviation in voltage level is the main objective to control [36], the use of smart inverters is being the best option. They will have a direct impact on users and consumers in the LV distribution network and be used with great flexibility under high PV penetration scenarios [37].

Inverters with reactive power capability are an interesting option [30–33]; however, the main disadvantages are not only the increase in the inverter nominal power to offer good performance but also an increment in the grid power losses and in the semiconductor stress, which entails a reduction in the useful life of the inverter.

In [31, 32], a static reactive power compensator is suggested and an analysis to select the best connection point is detailed. The main drawback of this work is that the proposal is no longer valid if the grid parameters change, like new loads and distribution transformer replacements.

In [38], coordinated hierarchal control of PV modules is discussed, which mitigates the voltage fluctuations using a smart control system; this system requires inverters with reactive power compensation capability, storage elements, and static synchronous compensators. The proposal is good to regulate the voltage; however, the disadvantages are the use of extra elements, increasing the complexity and cost.

Other works with extra elements are [39–41]; in [39], a multienergy storage system set is controlled through a complex communication network; in [40], a tapped transformer is considered, which should be a better solution than reactive power control because no extra current is handled, although the cost and complexity increase; in [41], a combination of tapped transformers and an energy storage system is proposed, and a particle swarm optimization is performed, resulting in a complex and expensive system; in [42], the use of electric vehicles by all consumers to ensure an efficient operation is considered, which is not practical in many regions and therefore a disadvantage.

In [43], a coordinated operation of a hybrid energy storage system (HESS) that can improve the utilization rate of PV systems is considered. A supercapacitor and a lithium battery are employed, coordinated with a complex particle swarm controller. Besides, the infrastructure involved in energy storage systems is large, which implies a high initial economic investment.

In this paper, a strategy to control a PV inverter is proposed, which allows reducing the voltage variations in an LV distribution network under a high PV penetration scenario through active power management. The proposal is simple because no extra elements are required, like tapped transformers, complex communication systems, electric vehicles, or energy storage systems. However, the use of an energy storage system is suggested, but optional to offer better characteristics.

The proposal does not consider either injecting/absorbing reactive power towards/from the grid. Only active power is managed; therefore, the power losses in the grid are not incremented and it is not required to oversize the inverter rated power. The proposal manages the active power delivered by the PV system depending on the grid conditions and the PV panel employing an algorithm that controls the PV inverter; therefore, there is no additional cost compared to the traditional PV system.

The proposed control strategy detects when a voltage variation is due to a high PV penetration scenario. This is an advantage compared to other methods that require the characterization of the complete grid to operate. The proposed strategy effectively mitigates voltage variations in the grid caused by high PV penetration and in addition achieves relevant functionalities for the system, such as the regulation of the DC bus voltage, maximum power point tracking (MPPT), grid voltage synchronization, the detection of high penetration conditions, and the active power strategy for the main controller.

The paper is organized as follows: Section 2 presents a simplified model of the LV distribution network considered. In Section 3, the effects of high PV penetration are shown, and the most critical configurations are illustrated. In Section 4, the proposed control strategy is detailed. The experimental results are shown in Section 5. Finally, the main conclusions are considered to resume the advantages and disadvantages of the proposed solution.

2. LV Distribution Network under High PV Penetration Scenario

For a better understanding of the high PV penetration phenomena, an LV distribution network is modeled. This illustrates the troubles associated with it in a simple way. It is assumed an axial grid connection since it is the most typical configuration in an LV distribution network in a resident area [44]. There are different grid configurations described in other works [14, 21, 45].

A typical residential cluster is considered, which is illustrated in Figure 1(a). The distribution network consists of the power transformer (v_g), residences (L_n), grid wiring (Z_n), and photovoltaic system (PV_n).

To simplify the analysis, some considerations and assumptions are made. The power injected by PV systems (PV_n) and residence load (L_n) are represented by a current source (i_n); both are considered sinusoidal. The transformer output (v_g) is replaced by a sinusoidal voltage source, and the grid impedances are equal (Z). The simplified circuit is shown in Figure 1(b).

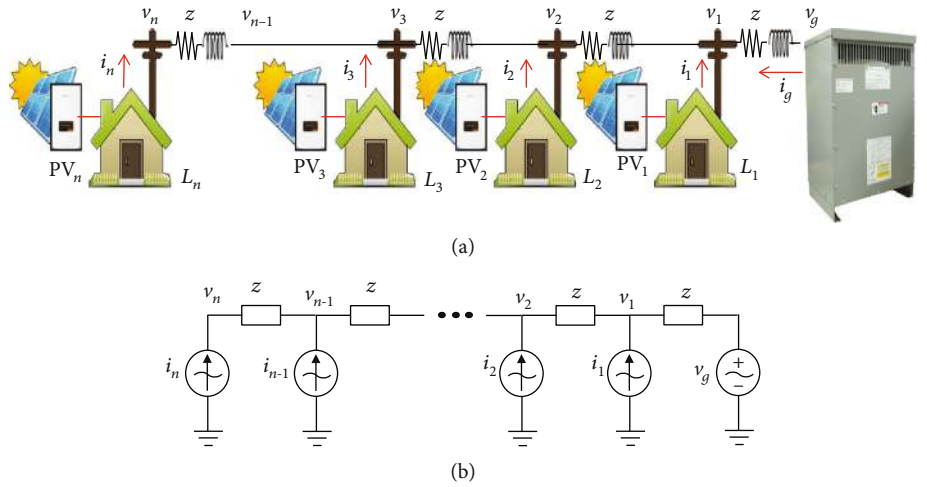

Figure 1: Analyzed system: (a) residential area with axial connection; (b) simplified circuit.

Analyzing the simplified circuit, it is obtained that

$$\begin{aligned} v_n &= v_{n-1} + Zi_n, \\ v_{n-1} &= v_{n-2} + Z(i_n + i_{n-1}), \\ &\vdots \\ v_1 &= v_g + Z(i_n + i_{n-1} + \cdots + i_1), \end{aligned} \tag{1}$$

where v_g is the transformer voltage, Z is the wiring impedance, n is the number of residences in the cluster, and i_n is the current that is injected into the grid from the residence point (n) according to its position.

The voltage in the n_{th} residence can be determined solving the equation system (1), as a function of current sources, giving

$$v_n = v_g + Z \sum_{m=1}^{n-1} (m \cdot i_m) + Zn \sum_{m=n}^{r} (i_m), \tag{2}$$

where n is the n_{th} residence in the cluster, and r is the number of residences.

Based on (2), a set of voltage equations that determine the voltage of each residence may be obtained. As an example, a distribution network consisting of 11 residences gives the following equations, for residences 1, 2, 5, 6, 10, and 11 which are, respectively,

$$v_1 = v_g + Z(i_1 + i_2 + \cdots + i_{10} + i_{11}), \tag{3}$$

$$v_2 = v_g + Z(i_1 + 2(i_2 + \cdots + i_{10} + i_{11})), \tag{4}$$

$$v_5 = v_g + Z(i_1 + 2i_2 + 3i_3 + 4i_4 + 5(i_5 + \cdots + i_{10} + i_{11})), \tag{5}$$

$$v_6 = v_g + Z(i_1 + 2i_2 + \cdots + 5i_5 + 6(i_6 + \cdots + i_{10} + i_{11})), \tag{6}$$

$$v_{10} = v_g + Z(i_1 + 2i_2 + \cdots + 9i_9 + 10(i_{10} + i_{11})), \tag{7}$$

$$v_{11} = v_g + Z(i_1 + 2i_2 + \cdots + 10i_{10} + 11i_{11}). \tag{8}$$

3. Grid Voltage Deviations under High PV Penetration Scenario

According to the mathematical model (2), the voltage variation in each residence depends on the actual injected/absorbed current towards/from the grid. Understanding the phenomenon will make it possible to establish a strategy to mitigate the harmful effects of high PV penetration.

A distribution network composed of 11 residences is used as an example. The parasitic elements of the grid are calculated considering the wiring impedance and the distance between residences, which is 11 m ($R_{\text{cable}} \approx 1.61\,\Omega$/km, $X_{L_{\text{cable}}} \approx 0.21\,\Omega$/km). The value of the current source i_n is calculated as the difference between the current delivered by each renewable source (I_{PV_n}) and the current demanded by each residence (I_{L_n}). The grid voltage is 120 V.

In Figure 2, the normalized voltages in six different residences (1, 2, 5, 6, 10, and 11) are shown. The sign of the current source (i_n) has been defined as positive if the renewable source generates more power than the one demanded by the residence; on the other hand, the current is negative if the residence demands more power than the one delivered by the renewable source. The vertical axis represents voltage while the horizontal axis represents time.

In Figure 2(a), the normalized voltage levels of the transformer and the residences are shown, and the current demanded by each residence is minus 4.4 A (residence plus PV system); then, the residences demand more energy than the PV systems deliver. The voltage in each residence is lower than the voltage of the transformer (v_g), and therefore, there is not an increment of the voltage grid.

In Figure 2(b), the voltage levels of the transformer and the residences are shown again, but now, the current delivered to the grid by each residence is 4.4 A (residence plus PV system); then, the residences demand less power than the PV system delivers. The voltage in each residence is now higher than the voltage of the transformer (v_g).

Figure 2(c) shows the same case as Figure 2(b), but the current is incremented to 8.8 A (residence plus PV system).

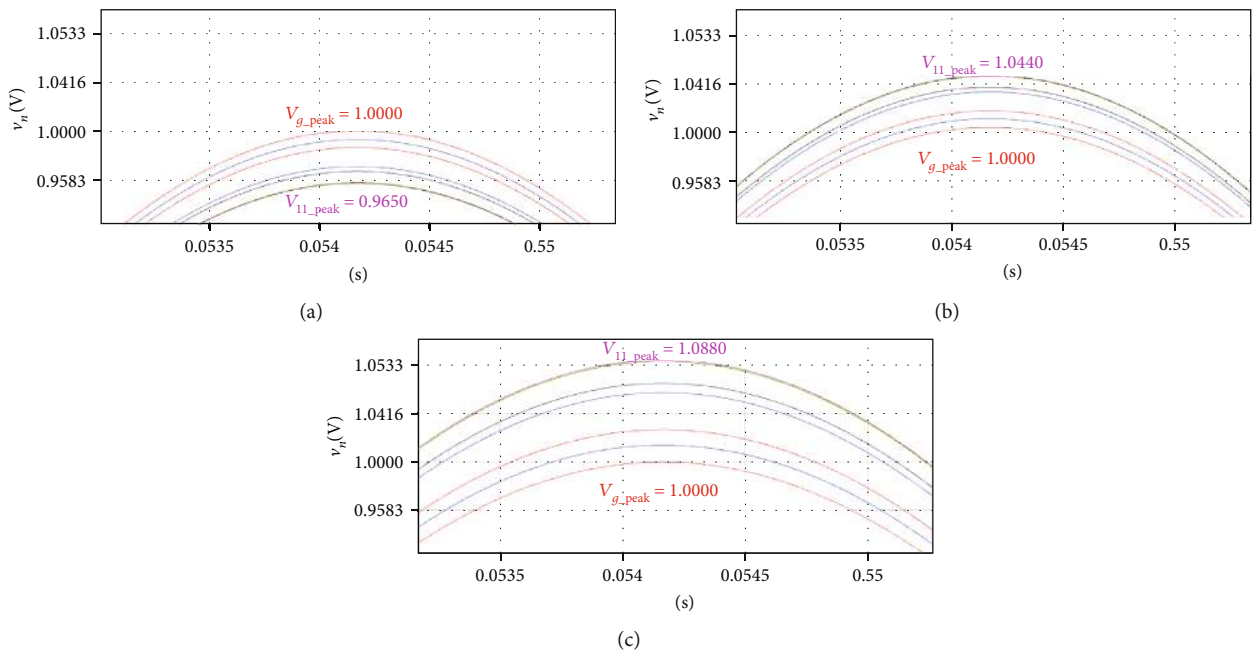

Figure 2: Voltage levels on the transformer and residences: (a) residences demanding power (-4.4 A), (b) residences injecting power (4.4 A), and (c) residences injecting power (8.8 A).

As it can be observed, the voltage in each residence is higher compared to the previous case, which may represent a load malfunction or damage due to the overvoltage. Moreover, it can be noticed that the umpteenth residence, which is the one farthest from the transformer, is the most affected since the voltage deviation is greater. Therefore, the umpteenth residence is the most critical in the distribution network.

Based on these observations, a control strategy for mitigating the harmful effects of high PV penetration is proposed. The active power delivered by the PV system may be appropriately managed once a voltage increment is detected due to a high PV penetration scenario, and then reduce the voltage increment to safe values.

4. Proposed System

Since the voltage fluctuation due to high PV penetration is caused by the grid parasitic elements and the inverse power injected by the PV system, in this paper, a power management strategy to alleviate the voltage variation is proposed. The reactive power compensation is not used to avoid oversizing the inverter rated power and to avoid wiring power losses. The proposed system is shown in Figure 3.

The power stage selected is the HERIC converter, suitable for PV applications [46]. This topology was selected because it offers good characteristics like lightweight (without transformer), low leakage current that satisfies the regulations, and high efficiency, and its operation and construction are similar with a traditional inverter, simplifying the implementation. The power stage is shown in Figure 3(a). However, any other topology with similar characteristics may be also used.

The proposed controller (Figure 3(b)), which manages the PV system power flow, consists of a proportional resonant (PR) current controller, a DC voltage regulator including an MPPT, a grid voltage synchronization stage, a high PV penetration detector (PD), the active power controller (APC), and finally an energy storage system (ESS). The latter, although optional, certainly improves the performance of the entire system.

For evaluating purposes, the proposed system is placed on the umpteenth residence since it is the most critical point, but it can be placed in another point. The other residences are considered as independent current sources, the wiring impedance is the same between the different residences, and the transformer voltage is considered as an independent voltage source. The power delivered by the residence PV system is managed to alleviate the local voltage fluctuation through the local grid injected current; the system changes the amplitude of the set point of the injected current.

4.1. Proportional Resonant Controller (PR). A proportional-integral (PI) control is commonly used for stationary or time-invariant references. However, when the reference has a sinusoidal shape, the PI control is not the best option, since a control that minimizes the steady-state error in sinusoidal variations and external disturbances is desirable. A PR control features an infinite gain, which eliminates the sinusoidal steady-state error at the operating frequency [47, 48].

The control law used is

$$G_c(s) = K_{\mathrm{p}}\left(1 + K_{\mathrm{r}}\frac{s}{s^2 + \omega_o^2}\right), \tag{9}$$

where K_{p} is the proportional constant, K_r is a controller constant, and ω_o is the resonance frequency.

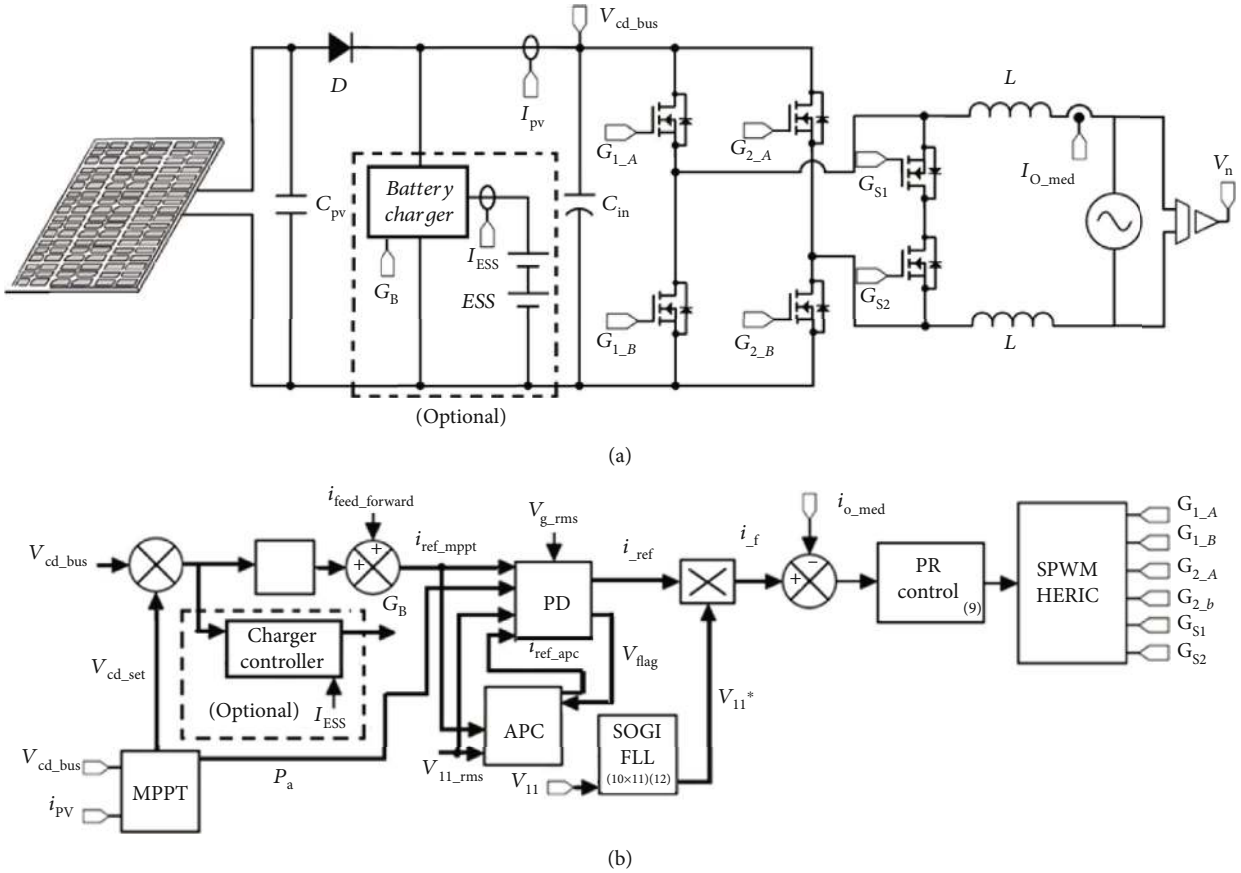

Figure 3: Proposed system: (a) power stage; (b) proposed controller.

Gain K_p is tuned to get the best dynamics of the system in terms of bandwidth but assuring stability with the proper phase and gain margins. Gain K_r is tuned to eliminate the steady-state error [48].

This controller allows obtaining the injected current as required by the APC or MPPT section. The K_p and K_r values are shown in Table 1. This type of controller employs averaged models, which assumes that the switching frequency may be neglected.

4.2. Voltage Synchronization. To synchronize the injected current with the local voltage, a second-order generalized integrator (SOGI) and a frequency locked loop (FLL) were used [49]. The equations used are

$$v_{11}^*(s) = \frac{k\omega_o s}{s^2 + \omega_o s + \omega_o^2} v_{11}(s), \tag{10}$$

$$v_{q11}^*(s) = \frac{k{\omega_o}^2}{s^2 + \omega_o s + \omega_o^2} v_{11}(s), \tag{11}$$

$$\omega_o = -\frac{\gamma}{s}(v_{11} - v_{11}^*)v_{q11}^*, \tag{12}$$

where k is a tuning constant, γ is a tuning constant, v_{11} is the input voltage (n_{th} residence), and v_{11}^* is the orthogonal synchronized output.

Table 1: Controller parameters.

Parameters	Units
K_p	2
K_r	10
k_i	1
k	1/170
Y	1

This section allows injecting the current synchronized with the voltage grid. For its implementation (Table 1), a value of k was selected to assure a normalized reference at nominal voltage to determine the current amplitude directly by the PD and γ is tuned to offer a good steady-state operation [49].

4.3. DC Bus Voltage Regulation and MPPT. When no voltage fluctuation occurs due to the high PV penetration, the PV system works traditionally; that is, the MPPT of the PV panel is tracked through the perturb and observe (P&O) algorithm [50]. The MPPT determines the voltage set point at the maximum power point, measuring the voltage and current of the PV panel.

To assure a low distortion in the injected current, the bandwidth of the voltage loop must be small; therefore, the

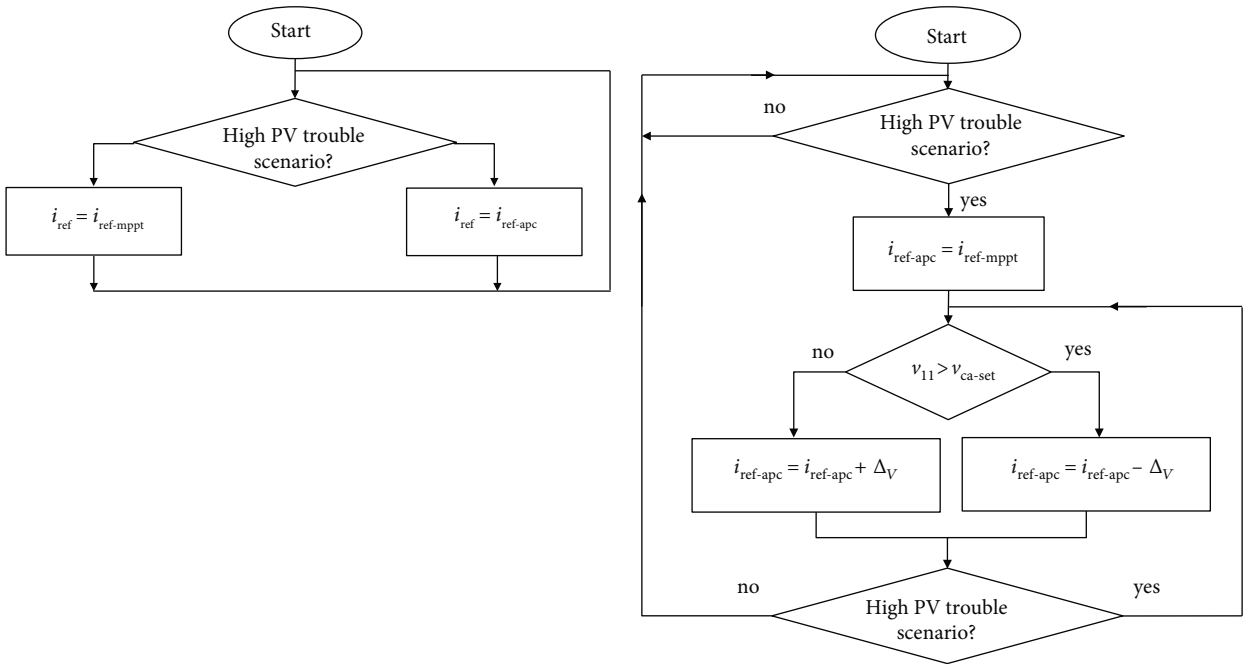

Figure 4: Flowchart: (a) penetration detector; (b) active power controller.

use of an integrator is enough to assure a good operation. Nevertheless, a feed-forward compensator is used to increase the fastness of the system under grid voltage variations, by using the actual power (P_a) of the PV panel to determine the current reference in a steady state. The equation used for the voltage controller is

$$i_{ref-mppt} = k_i \frac{v_{cd-bus} - V_{cd-set}}{s} + i_{feed-forward}. \quad (13)$$

The value of k_i was tuned to have a slow response, and then, to avoid distortion in the injected current, the bandwidth is selected ten times lower than 60 Hz.

4.4. High PV Penetration Detector (PD). To avoid the voltage fluctuations in a high PV penetration scenario, a PD is employed. This PD switches the operation between the MPPT voltage regulator and the APC (Figure 4(a)). The setpoint for the PR controller (i_{ref}) is set by the MPPT algorithm, in normal operation, or by the APC when a voltage increment is detected due to high PV penetration; additionally, it provides a flag that indicates the operating mode (V_{flag}).

To determine if there is voltage fluctuation due to high PV penetration, the voltage conditions are used. That is, if the local voltage is higher than the transformer voltage and above 5% of the nominal value, APC operations begin. If the local voltage is higher than the transformer voltage and below 4% of the nominal voltage, the MPPT voltage regulator is operating. This operating way allows extracting more power from the PV system when possible until the voltage is reasonably fulfilling the standard. According to the ANSI c84.1 standard, the maximum overvoltage allowed is 5.8%

Table 2: Experimental setup data.

Parameters/elements	Value
V_g	120 V @ 60 Hz
P_o	1 kW
L	4 mH
C_{in}	$2 \times 470\ \mu$F
MPPT algorithm	P&O
Proposed algorithm	APC
MOSFETs	C2M0160120D
Voltage sensor	LV25-P
Current sensor	LA25-NP
Digital platform	NI MyRIO 1900
Switching frequency of G_{1A}, G_{1B}, G_{2A}, G_{2B}	35 kHz
Switching frequency of G_{s1}, G_{s2}	60 Hz
DC bus voltage	250 V

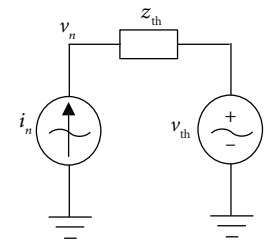

Figure 5: Simplified circuit.

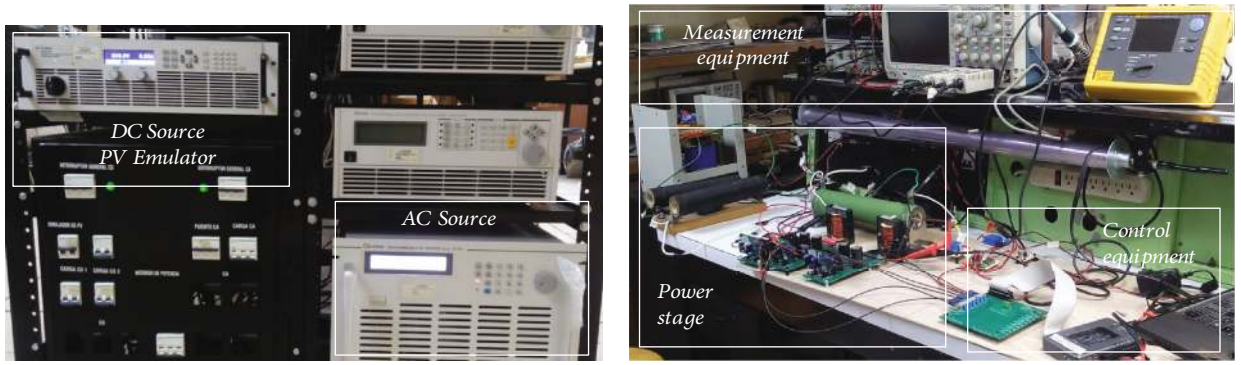

(a) (b)

Figure 6: Photography of the system: (a) power supplies; (b) power stage and controller.

above the nominal grid voltage, so it is assumed that the proposed voltage increment is acceptable for any residence. These two limits (5% and 4%) establish a hysteresis band, which determines the operation of the PD. Certainly; each limit may be adjusted according to other applicable standards in different regions.

The actual power of the PV panel (P_a) is considered to switch the operating mode from APC to MPPT since the APC delivers power regardless of the PV panel power availability. In case the PV panel cannot provide the power set by the APC, the MPPT voltage regulator must be selected instead of the APC.

4.5. Active Power Controller (APC). The APC goes into operation when it is detected that there are voltage fluctuations due to the high PV penetration. Then, the local voltage is regulated by changing the active power through the injected current.

Figure 4(b) shows the flowchart used to determine the APC current setpoint (i_{ref_apc}), which establishes the power injected into the grid during this mode. When a voltage increment due to a high PV penetration scenario occurs, the PD gives control to the APC. The initial current setpoint is the last current set point given by the MPPT algorithm ($i_{ref\_apc} = i_{ref\_mppt}$), and it is incremented or decremented according to the local voltage conditions to keep it regulated. If the local voltage at the residence is greater than the setpoint established ($V_{11} > V_{ca\_set}$), a decrease in the current reference is made, otherwise it is increased. Finally, the operating conditions are checked again to determine if whether the APC mode should be maintained or not.

The increment is given by an adaptive step, which is proportional to the absolute value of the voltage error. The ac voltage setpoint is selected as the center of the hysteresis band. Then, the equation used is

$$\Delta_V = K_{pe}|v_{11} - V_{ca\text{-}set}|, \tag{14}$$

where Δ_v is the increment, K_{pe} is the controller parameter, V_{11} is the local residence voltage, and V_{ca-set} is the reference for the regulated voltage.

This equation allows avoiding fluctuations in a steady state when the APC is operating.

4.6. Energy Storage System (ESS). The use of an ESS is suggested for a better performance of the system, but it is certainly optional, as it does not affect the voltage regulation on the ac side. If an ESS is not employed in a scenario where the APC is active, part of the energy available in the PV system is not injected into the grid and then dissipated by the PV system itself, which may affect the lifespan. Therefore, to improve the performance of the PV system, the energy that is not injected into the grid should be stored and when possible delivered to the grid or used for other types of applications.

In the case of using an ESS, a battery charger should be employed, which is enabled only in APC mode, the energy is taken from the DC bus voltage. The proposal of the charger controller is beyond the purpose of this work.

5. Experimental Validation

To verify that the proposed system operates properly and mitigate the voltage deviations in the ac grid, a laboratory prototype was built. Different tests were conducted to evaluate the performance of the proposed system: steady-state operation, startup, power variation in the renewable sources, distribution transformer voltage variations, and test under grid voltage distortion.

5.1. Workbench. For the tests, it is considered that the nominal grid voltage is 120 V (transformer voltage); the wiring impedances between residences are equal and have a value of $Z \approx 0.018\,\Omega$; the number of residences considered is 11, and the first 10 residences inject current to the grid but selectable to emulate the voltage fluctuations due to the high PV penetration. It is considered 100% of penetration, which means that all residences deliver power to the grid; to simplify the implementation, the same current is considered at each residence, but certainly, different power should be considered. The ANSI c84.1 standard is considered; then, the maximum allowed overvoltage is 5.8%, which is 126.96 V.

The proposed system is connected to the last residence, its PV system is working during the tests, but the last residence is not demanding energy to have the worst case. It is

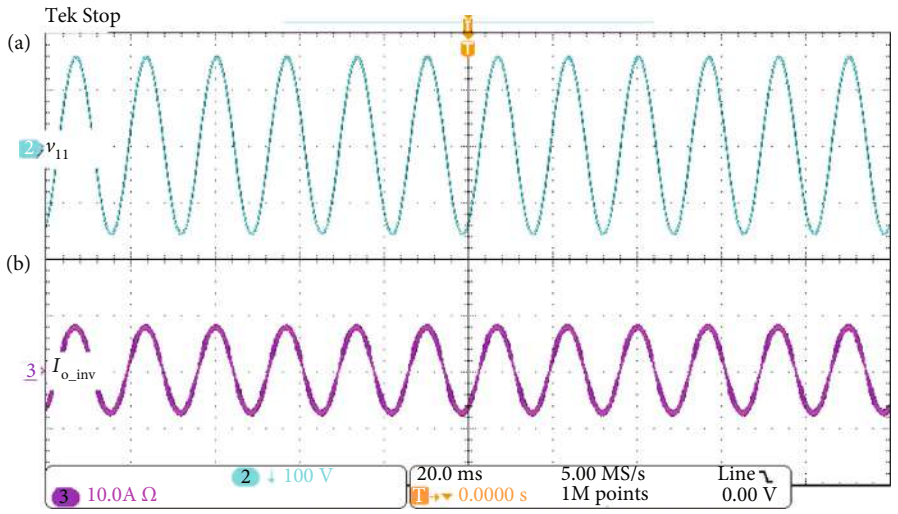

Figure 7: System operating at MPPT mode: (a) local voltage in residence 11 (V_{11}, 100 V/div); (b) current in residence 11 (I_{11}, 10 A/div). Time 20 ms/div.

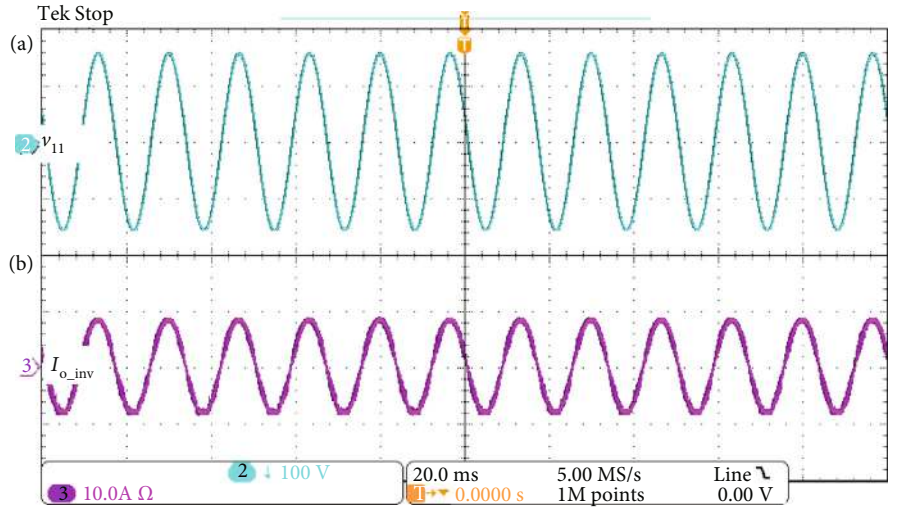

Figure 8: System operating at APC mode: (a) local voltage in residence 11 (V_{11}, 100 V/div); (b) current in residence 11 (I_{11}, 10 A/div). Time 20 ms/div.

considered that each PV system generates till 1 kW_p. The parameters of the implemented system are shown in Table 2.

To simplify the implementation, the Thévenin equivalent circuit of the first 10 residences is considered, resulting in the simplified circuit shown in Figure 5. Therefore, for the tests, only a single voltage source and impedance are used to emulate the first 10 residences.

The Thévenin voltage is

$$v_{\text{th}} = v_g + Z \sum_{m=1}^{r-1} (m i_m), \tag{15}$$

where r is the number of residences.

The Thévenin impedance is

$$Z_{\text{th}} = nZ. \tag{16}$$

To simplify the calculation of the Thévenin voltage, it is assumed that the injected current by each of the first 10 residences is equal, resulting in

$$v_{\text{th}} = v_g + Z i_{pv} \sum_{m=1}^{n-1} (m) = v_g + Z i_{pv} \frac{n(n-1)}{2}, \tag{17}$$

where i_{pv} is the injected current by the $n-1$ residences.

However, the experimental setup would be valid for any other configuration using (15) for the Thévenin voltage calculation.

A photograph of the implemented system is shown in Figure 6, where the ac power supply (Chroma 61703), the photovoltaic emulator (Keysight N8937APV), the power converter, the measurement equipment (oscilloscope Tek MSO3014 and power quality logger Fluke 1735), and the

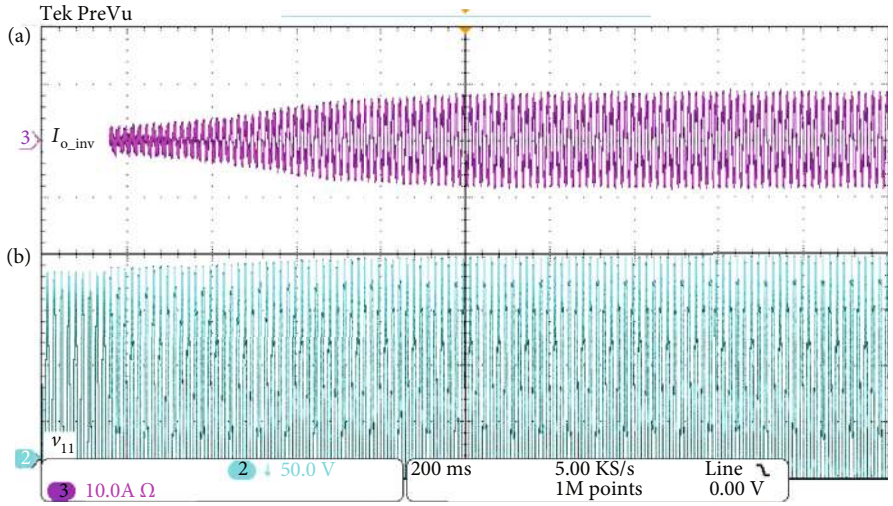

Figure 9: Startup: (a) current in residence 11 (I_{11}, 10 A/div); (b) local voltage in residence 11 (V_{11}, 50 V/div). Time 200 ms/div.

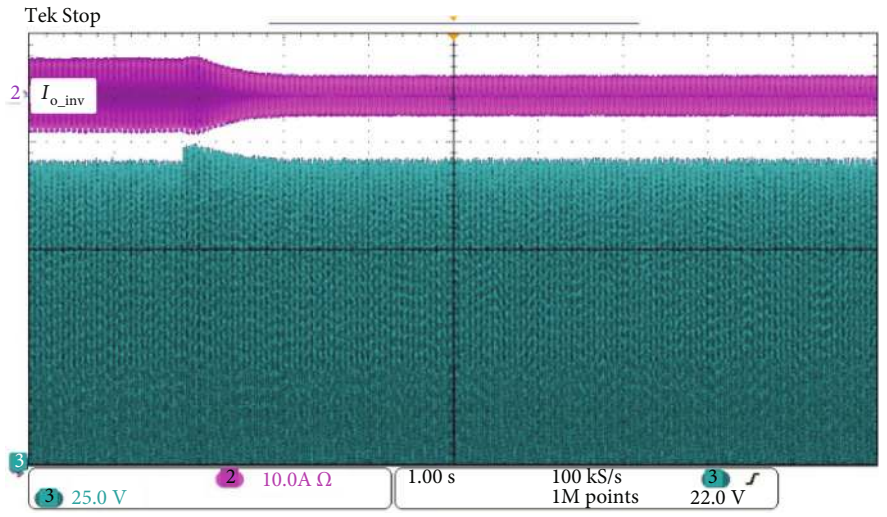

(a)

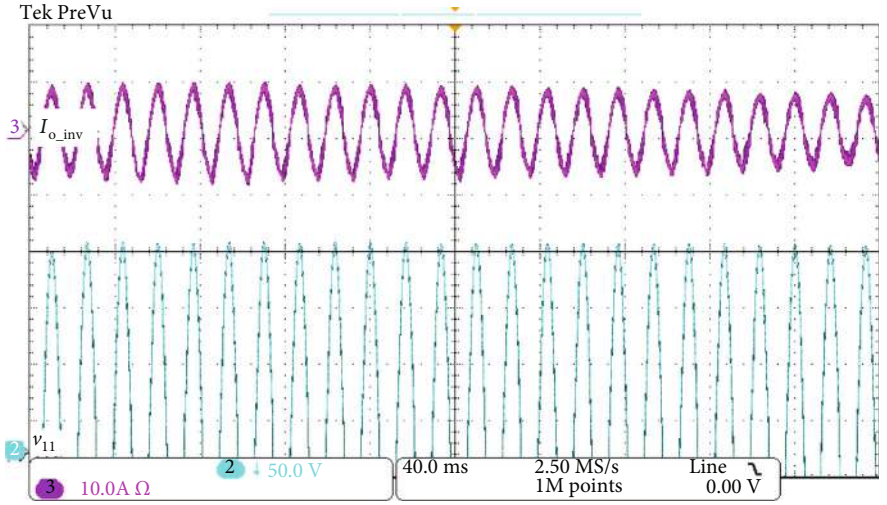

(b)

Figure 10: Power variation, for positive deviation. From top to bottom: current in residence 11 (I_{11}, 10 A/div), local voltage in residence 11 (V_{11}, 25 V/div). (a) Full transition, time 1 s/div; (b) zoom, time 40 ms/div.

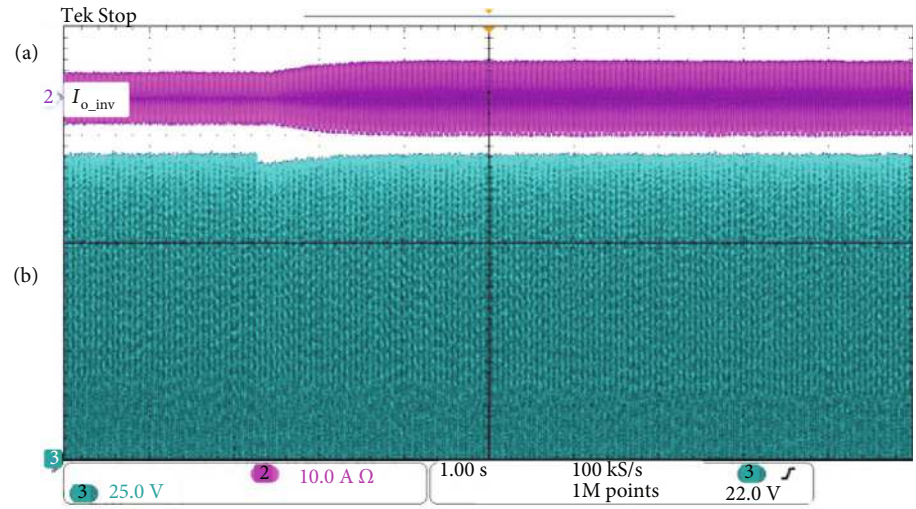

Figure 11: Power variation, for negative deviation: (a) current in residence 11 (I_{11}, 10 A/div); (b) local voltage in residence 11 (V_{11}, 25 V/div). Time 1 s/div.

control system employed (National Instruments myRIO 1900) can be observed.

Since the ac power supply cannot receive energy, otherwise it will be damaged, a dummy load is employed to emulate the electric grid. The energy that is injected is consumed by the dummy load; then, a safe test is made; this load is connected in parallel to the ac power supply.

5.2. Steady-State Operation. The proposed system offers a good steady-state operation due to the PR controller employed. In Figure 7, the voltage and current in residence 11 are shown, operating in MPPT mode. The current THD is 1.1%, and the PF is 0.99. Figure 8 shows the steady-state waveforms of voltage and current in residence 11, when the proposed system operates in the APC mode, thus regulating the voltage. The current THD is 1.2%, and the PF is 0.99. The leakage current is lower than 300 mAp in all cases, which complies with the VDE-0126-1-1 standard.

5.3. Startup. Figure 9 shows the injected current and the voltage in residence 11 during system startup. A smooth transition is performed when the system starts. The voltage of the evaluated residence is slightly affected by the grid impedance, so the voltage rises. For this test, the initial condition of the MPPT was set to have a fast transition.

5.4. Power Variation of PV Panels. To evaluate the dynamic performance of the proposal, power variations in the PV panels were performed. First, the current injected by the first 10 residences is increased. Second, the injected current by the first 10 residences is decreased. Finally, a third test is conducted with the PV system operating in a high PV penetration scenario without the APC and then enabling it. For all tests, the maximum voltage limit is set at 126 V, which is 0.8% below the value established by the ANSI c84.1 standard.

For the first two tests, the conditions given imply that there is a high PV penetration in the residential electrical grid, so that the APC algorithm comes into operation, maintaining the voltage in the last residence fulfilling the standard, according to the proposed operation. A sudden change in the injected current of the first 10 residences results in a fast voltage variation at the evaluated residence, which allows testing the dynamic response of the proposed system.

First, a positive deviation is performed (Figure 10). The injected current for the first 10 residences is incremented from 4 A to 6.7 A causing a voltage increment to 128 V at the residence under test, which is out of the standard limit. The proposed system begins to reduce the injected current to the point where the voltage is within standard limits. The injected current changes from an initial value of 7.1 A to approximately 3.5 A, in less than 1 s. Figure 10(a) shows the injected current and the voltage of residence under test; the time scale allows illustrating the voltage and current evolution. In Figure 10(b), a zoom is performed to illustrate the waveforms during the transition.

Second, a negative deviation is performed (Figure 11). The injected current by the first 10 residences is decremented from 4.2 A to 3.3 A, causing a voltage decrement to 124 V at the residence under test, which indicates that the PV system may inject more energy into the grid. The proposed system begins to increase the injected current to the point where the voltage is still within standard limits. The injected current changes from an initial value of 4.8 A to approximately 7 A, in less than 1 s. The figure shows the injected current and the voltage of the residence under test.

For the third test (Figure 12), a transition between operating modes is made. In the beginning, the prototype is working as a traditional PV system, regulating the injected current according to the MPPT, but in a high PV penetration scenario. This causes the voltage level at the residence under test to exceed the maximum limit allowed by the standard. Then, at a certain time, the proposed APC algorithm is enabled, which starts the modulation of the active power and reduces the local voltage within standard limits and according to the proposed operation.

5.5. Transformer Voltage Variation. To evaluate the performance of the proposal, distribution transformer voltage

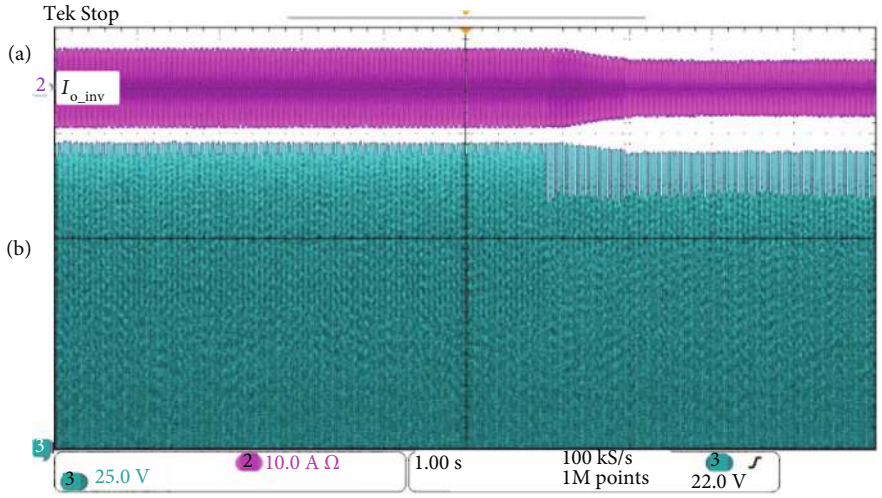

Figure 12: Transition from traditional MPPT and the proposed APC: (a) current in residence 11 (I_{11}, 10 A/div); (b) local voltage in residence 11 (V_{11}, 25 V/div). Time 1 s/div.

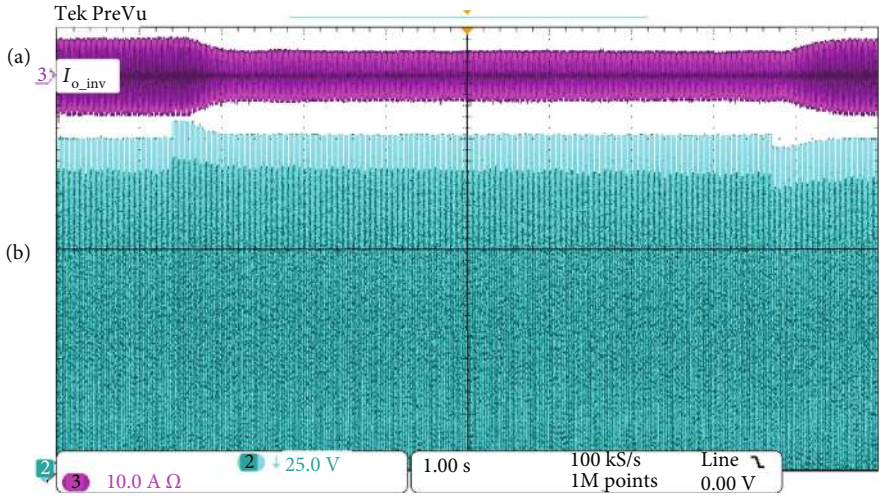

Figure 13: System response under transformer voltage variation (increment): (a) current in residence 11 (I_{11}, 10 A/div); (b) local voltage in residence 11 (V_{11}, 25 V/div). Time 1 s/div.

variation tests have been carried out. For these tests, the first 10 residences inject a constant current.

For the first test, it is considered that the last residence is operating in the APC mode. The initial transformer voltage is 120 V, suddenly increases to 125 V, and after 7 seconds approximately returns to 120 V. This is illustrated in Figure 13, where the local voltage and current at the 11th residence are shown. As it can be observed, during the first transition, the local voltage increases and the system reacts by injecting less power to regulate the voltage; in the second transition, the opposite behavior is observed while maintaining the voltage regulation.

The second test again considers that the last residence is operating in the APC mode, but now the transformer voltage drops suddenly from 120 V to 115 V and after 7 seconds returns to 120 V. This is illustrated in Figure 14, where the local voltage and current of the 11th residence are shown. As it can be observed, in the first transition, the local voltage decreases and the system reacts by injecting more power to regulate the voltage; in the second transition, the opposite behavior is shown while maintaining the voltage regulation.

5.6. Grid Voltage Distortion. Finally, a voltage distortion at the transformer voltage was imposed; since a synchronization circuit is employed, the injected current offers good performance. In Figure 15, the voltage and current at the last residence can be observed. The current THD is 1.4%, and the voltage THD is 5%. The transformer voltage distortion is also reflected in the evaluated residence. The proposal does not control the voltage waveform, and so the distortion remains at the voltage of residence under test.

5.7. Comparison Analysis. The proposed system is compared with other techniques; this is illustrated in Table 3. A methodology to design the grid under high PV penetration scenario is given in [24], which is a good alternative when the distribution system is a new design. However, for existing residential areas, the method is complex and expensive, and

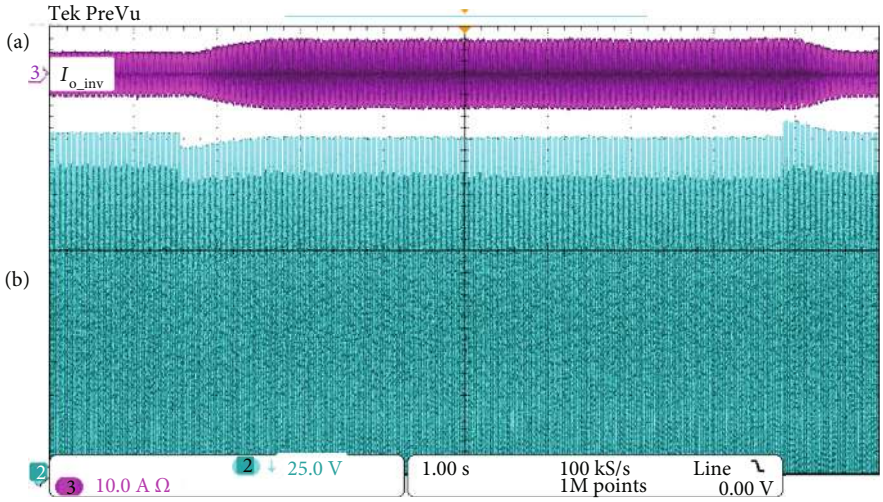

Figure 14: System response under transformer voltage variation (decrement): (a) current in residence 11 (I_{11}, 10 A/div); (b) local voltage in residence 11 (V_{11}, 25 V/div). Time 1 s/div.

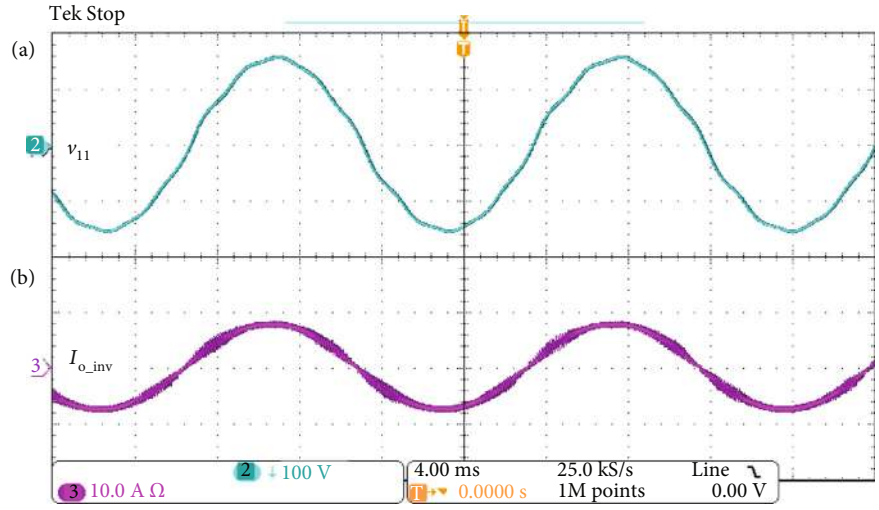

Figure 15: Grid voltage distortion test: (a) local voltage in residence 11 (V_{11}, 100 V/div); (b) current in residence 11 (I_{11}, 10 A/div). Time 4 ms/div.

in most cases, it would not be feasible due to the time and costs of the infrastructure modification. Then, it is not comparable with the proposed solution.

The use of variable tap transformers is proposed in [25]. The main advantage is that it is not invasive to the users; only a communication network may be added. The effectiveness of the proposal depends on the communication network and the number of taps in the transformer. There is still a possibility that depending on the grid conditions, the voltage variation may not keep within standard limits, resulting in a method that should be combined with other methods like the proposed in this work.

The use of ESS or electric vehicles may be a good alternative [27–29, 34]. This allows storing the PV energy; however, the ability to regulate the voltage variations depends on the storage capacity. That is, if the ESS is fully charged, the system may no longer compensate for the voltage variations, and therefore, the trouble may continue. This solution may be combined with other schemes to assure good operation.

In terms of cost (including power devices and controllers), it can be observed in Table 3 that the two best alternatives use a smart inverter with reactive power compensation [30–33] and the proposed strategy in this work. This is because no extra elements or devices or modifications on the infrastructure are required, just software modifications. However, if losses in the distribution grid are considered, our proposal becomes the better solution, since the injected current is not incremented for the reactive power compensation. Moreover, it is not necessary to increase the inverter power rate.

According to the experimental results (Figures 13 and 14), the settling time of the proposed system is less than 1 s, which is comparable with other techniques reported in the literature, but certainly, this time depends on the penetration detector not only on the proposed active power compensation.

Table 3: Strategy comparison to alleviate the high PV penetration troubles.

Reference/method	Advantages	Disadvantages	Complexity	Cost/economics	Setting time
[24]/grid design	Structured system and efficient No need for extra equipment and devices to mitigate high penetration	Only applicable for new residential areas under construction The phenomenon of high penetration may continue depending on grid conditions	High: although the method is desirable for residential areas under construction, its implementation can also be carried out in existing residential areas, which would involve complexity and cost	High: if the infrastructure already exists, it will imply high costs to make changes. On the other hand, if it is a new design, the solution would be cheaper.	Not applied
[25]/tapped transformer	Good for centralized and decentralized techniques It is not invasive for the users of the electrical network	The phenomenon of high penetration may continue, especially at critical points of connection Requires a bidirectional communication network	Low: exchange the transformer for one with variable tap	Medium: tapped transformer implies costs and also requires external communication components.	<0.3 s
[27–29]/energy storage	Store the energy not used in the moments of maximum PV generation. No losses at the PV system and then increase its lifespan	Not so ecological, due to the use of batteries Depending on the ESS capacity, the voltage variation may continue	Medium: extra stages and controllers are required	Medium: the batteries are expensive, and also a program for its maintenance is required.	≈0.3 s
[30–33]/reactive power	Good performance No extra infrastructure	Extra losses in wiring and inverter due to injection of reactive power The power inverter rated should be incremented In some cases, the grid must be characterized	Medium: in some cases, prior knowledge of critical points in the distribution system	Low: only software modifications are required, no extra infrastructure.	≈10 s
[33]/electric vehicles	Good performance Taking advantage of electric vehicles	For future implementation Extra infrastructure Synchronize users' times with cogeneration by PV systems	High: high logistics process to carry out the best use of the system	High: the cost of electrical or hybrid vehicles is high.	Not available
Proposed APC	No extra infrastructure No extra losses in the wiring network No increment on power inverter rated When batteries are employed, there are no losses at the PV system and then it increases its lifespan	If no batteries are employed, the PV MPPT is not reached when APC operates	Low: the implementation uses the same infrastructure of a traditional PV system	Low: only software modifications are required, no extra infrastructure. The use of batteries is suggested which may imply extra costs.	<1 s

The proposed method certainly is a good alternative that may reduce the voltage variations; however, the energy of the PV panel may be wasted or lost in the PV panel, which becomes its disadvantage. Therefore, the proposal may be combined with energy storage systems or tapped transformers to inject the most energy possible into the grid.

6. Conclusion

This paper presents a different solution to reduce voltage fluctuations in the power grid, caused by high PV penetration when a residential cluster is the load. The proposal uses the PV inverter to perform the voltage compensation, without

the need of extra devices or infrastructure. The active power is controlled instead of the reactive one, which permits the reduction of wiring and power converter losses but also avoids the increment of inverter nominal power.

The experimental results show that the proposed system is capable of reducing the voltage deviations in the power grid caused by high PV penetration. Tests were carried out under different conditions such as transformer voltage variations, PV panel variations, and voltage distortions, obtaining satisfactory results and keeping the voltage within the standard specifications. The proposal offers good characteristics compared to other schemes reported in the literature, which makes it competitive.

Certainly, the proposal has the drawback of not being able to harvest and inject all the energy available in the PV panels under all operating conditions, so it is suggested to combine the solution with energy storage systems or other methods.

Data Availability

The data used to support the findings of this study are included within the article.

Conflicts of Interest

The authors declare that there is no conflict of interest regarding the publication of this paper.

Acknowledgments

This work was supported in part by Tecnológico Nacional de México under project No. 10166.21-P.

References

[1] The Internal Energy Agency, 2021, http://www.iea.org.

[2] B. Ernst and B. Engel, "Grid integration of distributed PV-generation," in *2012 IEEE Power and Energy Society General Meeting*, pp. 1–7, San Diego, USA, 2012.

[3] V. Sharma, S. Mahfuzul, M. H. Haque, and T. Kauschke, "Effects of high solar photovoltaic penetration on distribution feeders and the economic impact," *Renewable and Sustainable Energy Reviews*, vol. 131, p. 110021, 2020.

[4] B. Matthiss, A. Momenifarahani, and J. Binder, "Storage placement and sizing in a distribution grid with high PV generation," *Energies*, vol. 142, 2021.

[5] B. Noone, *PV Integration on Australian Distribution Networks: Literature Review*, The Australian PV Association, UNSW, Australia, 2013, http://www.ceem.unsw.edu.au/sites/default/files/documents/APVA%20%20PV%20and%20DNSP%20Literature%20review%20September%202013.pdf.

[6] T. Aziz and N. Ketjoy, "PV penetration limits in low voltage networks and voltage variations," *IEEE Access*, vol. 5, pp. 16784–16792, 2017.

[7] N. Samaan, M. A. Elizondo, B. Vyakaranam et al., "Combined transmission and distribution test system to study high penetration of distributed solar generation," in *2018 IEEE/PES Transmission and Distribution Conference and Exposition (T&D)*, pp. 1–9, Denver, USA, 2018.

[8] K. A. Alboaouh and S. Mohagheghi, "Impact of rooftop photovoltaics on the distribution system," *Journal of Renewable Energy*, vol. 2020, 23 pages, 2020.

[9] T. Matsumura, M. Tsukamoto, A. Tsusaka et al., "Line-end voltage and voltage profile along power distribution line with large- power photovoltaic generation system," *International Journal of Photoenergy*, vol. 2019, 8 pages, 2019.

[10] K. Burges and J. Twele, "Power systems operation with high penetration of renewable energy - the German case," in *2005 International Conference on Future Power Systems*, pp. 1–5, Amsterdam, Netherlands, 2005.

[11] B. C. Ummels, M. Gibescu, E. Pelgrum, and W. L. Kling, "System integration of large-scale wind power in the Netherlands," in *2006 IEEE Power Engineering Society General Meeting*, pp. 1–8, Montreal, Canada, 2006.

[12] D. Infield and W. Lei, "The challenges of high wind energy penetration in the UK power system," in *2014 International Conference on Power System Technology*, pp. 2999–3003, Chengdu, China, 2014.

[13] I. Kouveliotis-Lysikatos, P. Kotsampopoulos, and N. Hatziargyriou, "Harmonic study in LV networks with high penetration of PV systems," in *2015 IEEE Eindhoven PowerTech*, pp. 1–6, Eindhoven, Netherlands, 2015.

[14] J. Hu, Z. Li, J. Zhu, and J. M. Guerrero, "Voltage stabilization: a critical step toward high photovoltaic penetration," *IEEE Industrial Electronics Magazine*, vol. 13, no. 2, pp. 17–30, 2019.

[15] O. Gandhi, D. S. Kumar, C. D. Rodríguez-Gallegos, and D. Srinivasan, "Review of power system impacts at high PV penetration Part I: factors limiting PV penetration," *Solar Energy*, vol. 210, pp. 181–201, 2020.

[16] S. Homan, N. Mac Dowell, and S. Brown, "Grid frequency volatility in future low inertia scenarios: challenges and mitigation options," *Applied Energy*, vol. 290, p. 116723, 2021.

[17] M. Karimi, H. Mokhlis, K. Naidu, S. Uddin, and A. H. A. Bakar, "Photovoltaic penetration issues and impacts in distribution network–A review," *Renewable and Sustainable Energy Reviews*, vol. 53, pp. 594–605, 2016.

[18] S. F. Kagadi and M. J. Prasad, "Impacts of high rooftop PV penetration in distribution network and its mitigation using DSTATCOM," in *7th International Conference on Electrical Energy Systems (ICEES)*, pp. 1–4, IEEE, Chennai India, 2021.

[19] C. Essayeh, M. R. El-Fenni, H. Dahmouni, and M. A. Ahajjam, "Energy management strategies for smart green microgrid systems: a systematic literature review," *Journal of Electrical and Computer Engineering*, vol. 2021, 21 pages, 2021.

[20] M. Thomson and D. G. Infield, "Network power-flow analysis for a high penetration of distributed generation," *IEEE Transactions on Power Apparatus and Systems*, vol. 22, no. 3, pp. 1157–1162, 2007.

[21] A. Lucas, "Single-phase PV power injection limit due to voltage unbalances applied to an urban reference network using real-time simulation," *Applied Sciences*, vol. 8, no. 8, p. 1333, 2018.

[22] G. Lv, Q. Wu, C. Wu, and C. XZG, "Dynamic parameters tracking and voltage sag source location in the distribution system with DG," in *2018 2nd IEEE Conference on Energy Internet and Energy System Integration (EI2)*, pp. 1–6, Beijing, China, 2018.

[23] S. Afonaa-Mensah, Q. W. Stephen, and B. B. Uzoejinwa, "Investigation of daytime peak loads to improve the power generation costs of solar-integrated power systems," *International Journal of Photoenergy*, vol. 2019, 2019.

[24] R. A. Shayani and M. Oliveira, "Photovoltaic generation penetration limits in radial distribution systems," *IEEE Transactions on Power Systems*, vol. 26, no. 3, pp. 1625–1631, 2011.

[25] Y. Liu, J. Bebic, B. Kroposki, J. de Bedout, and W. Ren, "Distribution system voltage performance analysis for high-penetration PV," in *2008 IEEE Energy 2030 Conference*, pp. 1–8, Atlanta, USA, 2008.

[26] D. Das, V. M. Hrishikesan, C. Kumar, and M. Liserre, "Smart transformer-enabled meshed hybrid distribution grid," *IEEE Transactions on Industrial Electronics*, vol. 68, no. 1, pp. 282–292, 2021.

[27] A. Alzahrani, H. Alharthi, and M. Khalid, "Minimization of power losses through optimal battery placement in a distributed network with high penetrations of photovoltaics," *Energies*, vol. 13, no. 1, pp. 1–16, 2020.

[28] N. Mahmud, A. Zahedi, and A. Mahmud, "A cooperative operation of novel PV inverter control scheme and storage energy management system based on ANFIS for voltage regulation of grid-tied PV system," *IEEE Transactions on Industrial Informatics*, vol. 13, no. 5, pp. 2657–2668, 2017.

[29] Y. Xing, H. Zhao, Z. Shen et al., "Optimal coordinated energy management in active distribution system with battery energy storage and price-responsive demand," *Mathematical Problems in Engineering*, vol. 2021, 12 pages, 2021.

[30] A. Singhal, V. Ajjarapu, J. Fuller, and J. Hansen, "Real-time local volt/var control under external disturbances with high PV penetration," *IEEE Transactions on Smart Grid*, vol. 10, no. 4, pp. 3849–3859, 2019.

[31] M. Hasheminamin, V. G. Agelidis, A. Ahmadi, P. Siano, and R. Teodorescu, "Single-point reactive power control method on voltage rise mitigation in residential networks with high PV penetration," *Renewable Energy*, vol. 119, pp. 504–512, 2018.

[32] S. Ouali and C. Abdeljabbar, "Elimination of the impact produced by DG units on the voltage profile of distribution networks," *Journal of Applied Mathematics*, vol. 2020, 8 pages, 2020.

[33] S. Singh, V. B. Pamshetti, A. K. Thaur, and S. P. Singh, "Multistage multiobjective volt/var control for smart grid-enabled CVR with solar PV penetration," *IEEE Systems Journal*, pp. 1–12, 2021.

[34] A. Ali, D. Raisz, and K. Mahmoud, "Mitigation of voltage fluctuation in distribution system connected with PV and PHEVs using artificial bee colony algorithm," in *2018 6th International Istanbul Smart Grids and Cities Congress and Fair (ICSG)*, pp. 144–148, Istanbul, Turkey, 2018.

[35] M. Chamana, B. Chowdhury, and F. Jahanbakhsh, "Distributed control of voltage regulating devices in the presence of high PV penetration to mitigate ramp-rate issues," *IEEE Transactions on Smart Grid*, vol. 9, no. 2, pp. 1086–1095, 2018.

[36] J. A. P. Lopes, N. Hatziargyriou, J. Mutale, P. Djapic, and N. Jenkins, "Integrating distributed generation into electric power systems: a review of drivers, challenges and opportunities," *Electric Power Systems Research*, vol. 77, no. 9, pp. 1189–1203, 2007.

[37] J. Matevosyan, B. Badrzadeh, and T. Prevost, "Grid-forming inverters: are they the key for high renewable penetration?," *IEEE Power and Energy Magazine*, vol. 17, no. 6, pp. 89–98, 2019.

[38] F. Rafi, H. M. Hossain, and J. Lu, "Hierarchical controls selection based on PV penetrations for voltage rise mitigation in a LV distribution network," *International Journal of Electrical Power & Energy Systems*, vol. 81, pp. 123–139, 2016.

[39] P. Yu, C. Wan, Y. Song, and Y. Jiang, "Distributed control of multi-energy storage systems for voltage regulation in distribution networks: a back-and-forth communication framework," *IEEE Transactions on Smart Grid*, vol. 12, no. 3, 2021.

[40] T. Aziz and N. Ketjoy, "Enhancing PV penetration in LV networks using reactive power control and on load tap changer with existing transformers," *IEEE Access*, vol. 6, pp. 2683–2691, 2018.

[41] R. Zafar, J. Ravishankar, and H. R. Pota, "Centralized control of step voltage regulators and energy storage system under high photovoltaic penetration," in *2016 IEEE Innovative Smart Grid Technologies - Asia (ISGT-Asia)*, pp. 511–516, Melbourne, Australia, 2016.

[42] E. Vega-Fuentes and M. Denai, "Enhanced electric vehicle integration in the UK low-voltage networks with distributed phase shifting control," *IEEE Access*, vol. 7, pp. 46796–46807, 2019.

[43] D. L. Zhang, J. B. Guo, and J. L. Li, "Coordinated control strategy of hybrid energy storage to improve accommodating ability of PV," *The Journal of Engineering*, vol. 2017, no. 13, pp. 1555–1559, 2017.

[44] E. Mandefro Getie, G. Belachew Bantyirga, and T. Gera Workneh, "Photovoltaic generation integration with radial feeders using GA and GIS," *International Journal of Photoenergy*, vol. 2020, 7 pages, 2020.

[45] M. G. Kashani, S. Bhattacharya, J. Matamoros, D. Kaiser, and M. Cespedes, "Autonomous inverter voltage regulation in a low-voltage distribution network," *IEEE Transactions on Smart Grid*, vol. 9, no. 6, pp. 6909–6917, 2018.

[46] P. Somani and D. Vaghela, "Design of HERIC configuration based grid-connected single-phase transformerless photovoltaic inverter," in *2016 International Conference on Electrical, Electronics, and Optimization Techniques (ICEEOT)*, pp. 892–896, Chennai, India, 2016.

[47] G. Shen, X. Zhu, J. Zhang, and D. Xu, "A new feedback method for PR current control of LCL-filter-based grid-connected inverter," *IEEE Transactions on Industrial Electronics*, vol. 57, no. 6, 2010.

[48] R. Teodorescu, F. Blaabjerg, U. Borup, and M. Liserre, "A new control structure for grid-connected LCL PV inverters with zero steady-state error and selective harmonic compensation," in *Nineteenth Annual IEEE Applied Power Electronics Conference and Exposition, 2004. APEC 04*, pp. 580–586, Anaheim, USA, 2004.

[49] H. Yi, X. Wang, F. Blaabjerg, and F. Zhuo, "Impedance analysis of SOGI-FLL-based grid synchronization," *IEEE Transactions on Power Electronics*, vol. 32, no. 10, pp. 7409–7413, 2017.

[50] N. Khaehintung, T. Wiangtong, and P. Sirisuk, "FPGA implementation of MPPT using variable step-size P&O algorithm for PV applications," in *2006 International Symposium on Communications and Information Technologies*, pp. 212–215, Bangkok, Thailand, 2006.